Single GUV Method Reveals Interaction of Tea Catechin (−)-Epigallocatechin Gallate with Lipid Membranes

Yukihiro Tamba,* Shinya Ohba,† Masayo Kubota,‡ Hiroe Yoshioka,‡ Hisashi Yoshioka,¶ and Masahito Yamazaki*†§

*Innovative Joint Research Center, Shizuoka University, Hamamatsu 432-8011, Japan; †Department of Physics, Faculty of Science, ‡Radiochemical Research Laboratory, Faculty of Science, and §Integrated Bioscience Section, Graduate School of Science and Technology, Shizuoka University, Shizuoka 422-8529, Japan; and ¶Institute for Environmental Sciences, Shizuoka University, Shizuoka 422-8526, Japan

ABSTRACT Tea catechins, which are flavonoids and the main components of green tea extracts, are thought to have antibacterial and antioxidant activity. Several studies indicate that lipid membranes are one of the targets of the antibacterial activity of catechins. Studies using a suspension of large unilamellar vesicles (LUVs) indicate that catechin causes gradual leakage of internal contents from LUVs. However, the detailed characteristics of the interaction of catechins with lipid membranes remain unclear. In this study, we investigated the interaction of (−)-epigallocatechin gallate (EGCg), a major catechin in tea extract, with single giant unilamellar vesicles (GUVs) of egg phosphatidylcholine (egg PC) using phase-contrast fluorescence microscopy and the single GUV method. We prepared GUVs of lipid membranes of egg PC in a physiological ion concentration (~150 mM NaCl) using the polyethylene glycol-lipid method. Low concentrations of EGCg at and above 30 μM induced rapid leakage of a fluorescent probe, calcein, from the inside of single egg PC-GUVs; after the leakage, the GUVs changed into small lumps of lipid membranes. On the other hand, phase-contrast microscopic images revealed the detailed process of the EGCg-induced burst of GUVs, the decrease in their diameter, and their transformation into small lumps. The dependence of the fraction of burst GUVs on EGCg concentration was almost the same as that of the fraction of leaked GUV. This correlation strongly indicates that the leakage of calcein from the inside to the outside of the GUV occurred as a result of the burst of the GUV. The fraction of completely leaked GUV and the fraction of the burst GUV increased with time and also increased with increasing EGCg concentration. We compared the EGCg-induced leakage from single GUVs with EGCg-induced leakage from a LUV suspension. The analysis of the EGCg-induced shape changes shows that the binding of EGCg to the external monolayer of the GUV increases its membrane area, inducing an increase in its surface pressure. Small angle x-ray scattering experiments indicate that the intermembrane distance of multilamellar vesicles of PC membrane greatly decreased at EGCg concentrations above the threshold, suggesting that neighboring membranes came in close contact with each other. On the basis of these results, we discuss the mechanism of the EGCg-induced bursting of vesicles.

INTRODUCTION

Tea catechins are flavonoids and are the main components of green tea extracts. Some tea catechins have been found to have antibacterial activity (e.g., against *Streptococcus mutans* (a cariogenic bacterium), methicillin-resistant *Staphylococcus aureus*, and *Helicobacter pylori*) (1–4), antioxidant activity, or free radical scavenging activity (4–7). (−)-Epigallocatechin gallate (EGCg) (Fig. 1) is the most abundant catechin in tea extract (1). Several studies indicate that catechins bind to lipid membranes and that lipid membranes are one of the targets of the antibacterial activity of catechins (8–14). Many researchers have reported that catechins induce leakage of small fluorescent probes such as calcein and carboxyfluorescein from the inside of large unilamellar vesicles (LUVs) and small unilamellar vesicles (SUVs) of phosphatidylcholine (PC) membranes, indicating that catechins cause damage to the lipid membranes (8–12). However, there have been no detailed studies of the interaction of catechins with the lipid membranes and the mechanism of catechin-induced leakage of the internal contents of vesicles.

Recently, giant unilamellar vesicles (GUVs) of lipid membranes with a diameter of $\geq$10 μm have attracted much attention from researchers. Physicists and biophysicists have used GUVs to study physical properties of vesicle membranes such as elasticity and shape change (e.g., 15–20). The shape of a single GUV and its physical properties in water can be measured in real time. Thus, GUVs have a great advantage over smaller liposomes such as LUVs and SUVs in studies of physical properties and structural changes of liposomes. On the other hand, in the field of biochemistry of biomembranes, all studies of liposomes have been conducted using a suspension of many small liposomes, such as SUVs and LUVs, and various physicochemical methods, such as light scattering, fluorescence spectroscopy, electron spin resonance, and x-ray scattering. In those studies, the average values of the physical parameters of liposomes were obtained from a large number of liposomes, and thereby much information was lost. In contrast, studies of single GUVs provide information on the structure and physical properties of single GUVs as a function of time and spatial coordinates, and the statistical analysis of the physical properties of many single

Submitted September 8, 2006, and accepted for publication January 4, 2007.

Address reprint requests to Dr. Masahito Yamazaki, Integrated Bioscience Section, Graduate School of Science and Technology, Shizuoka University, 836 Oya, Suruga-ku, Shizuoka 422-8529, Japan. Tel./Fax: 81-54-238-4741; E-mail: spmyama@ipc.shizuoka.ac.jp.

0006-3495/07/05/3178/17 $2.00

doi: 10.1529/biophysj.106.097105

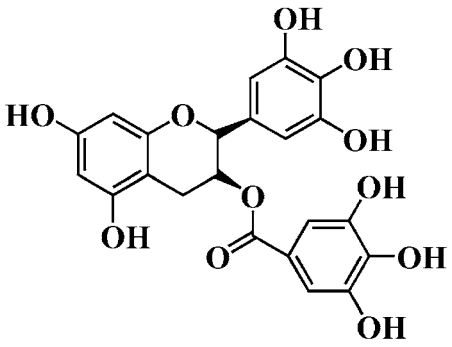

FIGURE 1 Chemical structure of EGCg.

GUVs can provide a great deal of new information on the structure and function of biomembranes and lipid membranes which cannot be obtained from studies using suspensions of LUVs and SUVs (the single GUV method) (21). For example, the single GUV method has been successfully used to study membrane fusion and vesicle fission (22,23).

The measurement of leakage of internal contents (such as small fluorescent probes) from liposomes in suspensions of many SUVs or many LUVs has been extensively used to investigate their interaction with various kinds of substances, including drugs, antibacterial substances, and fusogens, which induce membrane fusion of vesicles (the conventional LUV suspension method) (e.g., 24–26). A large amount of leakage indicates that the substance strongly interacts with lipid membranes, inducing instability in the structure of vesicles and lipid membranes. However, in the conventional LUV suspension method, we could not determine the main cause of the leakage because there are many possible factors that could be involved in the leakage, e.g., instability of membrane structure due to large deformation of vesicles or membrane fusion, formation of a narrow pore or ion channels, and disruption of vesicles. In one previous study (27), we investigated the interaction of the antimicrobial peptide magainin 2 with lipid membranes, using the single GUV method. Before that study, many researchers had reported that magainin 2 induced gradual leakage of internal contents from liposomes over a 10–20 min period, based on leakage experiments using a suspension of many LUVs (25,26). We found that low concentrations ($3-10\ \mu$M) of magainin 2 induced rapid leakage of a fluorescent probe, calcein, from the inside of single GUVs without disruption of the liposomes or changes in their membrane structure, indicating that magainin 2 formed pores in the membrane through which calcein leaked. The rapid leakage of the fluorescent probe from a GUV started stochastically, and once it began, the complete leakage occurred rapidly within ~1 min. This result indicates that the pore formation is the rate-determining step, rather than the leakage through the pore. These findings suggest that the increase in the fraction of completely leaked liposomes with time is responsible for the gradual increase in the leakage from the suspension of many LUVs over time. Using the single GUV method, we obtained much new information on the magainin 2-induced leakage of the internal contents, showing that the single GUV method is a promising method for investigation of leakage of the internal contents of vesicles and the interaction of substances with lipid membranes (27).

In this study, we investigated the interaction of EGCg with PC membranes using the single GUV method. Many researchers have found, based on leakage experiments using a suspension of many LUVs or SUVs, that EGCg and other tea catechins induce a gradual leakage of small fluorescent probes from the inside of liposomes (8–10). We expected that the single GUV method would produce new information on the interaction of EGCg with lipid membranes. For this study, we prepared GUVs composed of PC membranes in the liquid-crystalline phase in a physiological ion concentration (~150 mM NaCl), using the polyethylene glycol (PEG)-lipid method (28). Low concentrations of EGCg induced rapid leakage of a fluorescent probe, calcein, from the inside of single egg PC-GUVs. We found that this leakage occurred due to the bursting of the GUV. We compared EGCg-induced leakage from single GUVs with EGCg-induced leakage from the LUV suspension. The analysis of the EGCg-induced shape changes showed that binding of EGCg to the external monolayer of the GUV increases its membrane area, inducing an increase in its surface pressure. On the basis of these results, we discuss the mechanism of the EGCg-induced bursting of vesicles.

MATERIALS AND METHODS

Materials

Egg PC was purchased from NOF Corp. (Tokyo, Japan). 1,2-Dioleoyl-*sn*-glycero-3-phosphocholine (DOPC) and 1,2-dioleoyl-*sn*-glycero-3-phosphoethanol-amine-*N*-[poly(ethylene glycol) 2000] (PEG2K-DOPE) were purchased from Avanti Polar Lipids (Alabaster, AL). EGCg was purchased from Nagara Science Corp. (Gifu, Japan). Calcein was purchased from Dojindo Laboratory (Kumamoto, Japan). Bovine serum albumin (BSA) and cholesterol were purchased from Wako Pure Chemical Industry (Osaka, Japan).

Formation and microscopic observation of GUVs

Using the PEG-lipid method that we previously developed (28), we prepared GUVs of egg PC membrane (egg PC-GUV) in a buffer containing 150 mM NaCl, exploiting the natural swelling of a dry lipid film at 37°C, as follows. We put 100 μl of a 1 mM phospholipid mixture (egg PC/PEG-lipid; molar ratio, 99:1) in chloroform in a glass vial (5 ml) and dried it under a stream of N_2 gas to produce a thin, homogeneous lipid film. The solvent was completely removed by keeping the bottle containing the dry lipid film in a vacuum desiccator connected to a rotary vacuum pump for more than 12 h. Next, 10 μl of water was added into the glass vial, and the mixture was incubated at 45°C for 10 min (prehydration). The hydrated lipid film was then incubated with 1 ml of buffer H (10 mM HEPES, pH 7.4, 150 mM NaCl) containing 0.1 M sucrose or 1 ml of 1 mM calcein in buffer H containing 0.1 M sucrose for 2–3 h at 37°C. Untrapped calcein was removed as described in our previous report (27), as follows. The GUV suspension was centrifuged at $14{,}000 \times g$ for 10 min at 20°C to remove multilamellar vesicles (MLVs). The supernatant was collected and passed through a

Sephadex G-75 column with buffer H containing 0.1 M glucose, and the fractions containing GUVs were collected.

A 10-μl aliquot of the GUV solution (containing 0.1 M sucrose solution; internal solution) was diluted into 290 μl of 0.1 M glucose in buffer H (external solution), and this solution was transferred into a handmade microchamber (19,27). A slide glass was coated with 0.1% (w/v) BSA in buffer H containing 0.1 M glucose. We observed GUVs using an inverted fluorescence phase contrast microscope (IX-70, Olympus, Tokyo, Japan) at room temperature (22°C ± 2°C). Phase contrast images and fluorescence images of GUVs were recorded using a charge-coupled device camera (DXC-108, Sony, Tokyo, Japan) with a video recorder. The fluorescence intensity inside of GUVs was measured using Image J (Ver.1.33u; National Institutes of Health, Bethesda, MD) (29), and the average intensity per GUV was estimated. As GUVs, we selected vesicles whose membranes had a low contrast and a high undulation motion. Various concentrations of EGCg in buffer H containing 0.1 M glucose were introduced slowly into the vicinity of a GUV via a glass micropipette (diameter, 20 μm) positioned by a micromanipulator. The details of this method are described in our previous reports (23,27).

Formation of LUVs and interaction of EGCg with egg PC-LUVs

LUVs of egg PC or egg PC/PEG-lipid (molar ratio, 99:1) were prepared by the extrusion method using membranes with 200-nm pores (27). The appropriate amounts of lipids in chloroform were mixed and dried under a stream of N_2 gas, after which the solvent was completely removed by keeping the sample in a vacuum desiccator connected to a rotary vacuum pump for more than 12 h. To prepare MLVs, 1 ml of 70 mM calcein in water (pH 7.4; adjusted with NaOH) was added to the dry lipid film, and the suspension was vortexed several times for ~30 s at room temperature. Next, the suspension of MLVs was subjected to five cycles of freezing in liquid N_2 for 2 min, followed by thawing at room temperature for 20 min (freeze-thawing). The resulting solution was extruded through a membrane (pore size, 200 nm) using a LF-1 LiposoFast apparatus (Avestin, Ottawa, Canada) until the solution became transparent. To remove the untrapped calcein, the LUV suspension was passed through a Sephadex G-75 column equilibrated with buffer H. A Hitachi F3000 spectrofluorimeter (Hitachi, Tokyo, Japan) was used to perform the fluorescence measurements. Fluorescence intensities of samples were measured at room temperature. The excitation wavelength was 490 nm, and the emission wavelength was 520 nm. The excitation and emission band passes were 1.5 nm. We mixed the LUV suspension with various concentrations of EGCg solution and transferred the mixtures into a cell for the fluorescence measurement. During the measurement of the time course of the fluorescence intensity, we stirred the samples using a stirrer bar in the cell. The concentration of total phospholipids in the samples used for fluorescence measurements was 56 μM, as determined by the Bartlett method. The fluorescence intensity of the egg PC-LUV suspension in the absence of EGCg and in the presence of 0.6% (v/v) Triton X-100 were designated as 0% and 100% leakage, respectively.

For the measurement of the association of LUVs in the presence of EGCg, we prepared egg PC-LUVs in buffer H using the method described above. To get information on the effect of EGCg on the light scattering of the LUV suspension, absorbance of the LUV suspensions in the presence of various concentrations of EGCg was measured at 500 nm using a Spectrophotometer UV-1200 (Shimadzu, Kyoto, Japan). The concentration of total phospholipids in the samples used for light scattering measurements was 61 μM, as determined by the Bartlett method.

Determination of partition coefficient of EGCg from the aqueous solution into the lipid membrane using a suspension of egg PC-LUVs

Egg PC-LUVs were prepared in buffer H using the method described above. A Hitachi F3000 spectrofluorimeter was used for fluorescence measurements. Fluorescence intensities of samples were measured at room temperature. The excitation wavelength was 276 nm, and the emission wavelength was 355 nm. The excitation and emission band passes were 5 nm. The concentration of total phospholipids in the samples used for fluorescence measurements was determined by the Bartlett method. The method used to determine the partition coefficient is described in the Results and Discussion section. The fluorescence intensity of EGCg in the presence of egg PC-LUVs, $F([L])$, was obtained by subtracting the fluorescence intensity of the same egg PC-LUV suspension in the absence of EGCg.

Preparation of MLV and small angle x-ray scattering measurement

MLVs of DOPC membranes were prepared as follows (30). DOPC dissolved in chloroform was dried by N_2 and was then kept under vacuum provided by a rotary vacuum pump for >12 h. Appropriate amounts of buffer H containing a given concentration of EGCg were added to the dry film of DOPC under excess water conditions. Then, the suspensions were vortexed several times for ~20 s each time at room temperature (~22°C). To attain equilibrium, we freeze-thawed samples; after the vortexing, these suspensions were frozen in liquid N_2 for 2 min and were then thawed at room temperature for 30 min. This freeze-thawing was repeated four times to equilibrate the suspensions. For measurements of x-ray diffraction, we used pellets obtained from centrifugation (12,000 × g, 50 min at 20°C; Tomy, MR-150) of the lipid suspensions. X-ray diffraction experiments were performed using nickel-filtered Cu K_α x-rays ($\lambda = 0.154$ nm) produced by a rotating anode x-ray generator (Rigaku, Tokyo, Japan, Rotaflex, RU-300) under standard operating conditions (40 kV × 200 mA). Small angle x-ray scattering (SAXS) data were recorded using a linear (one-dimensional) position-sensitive proportional counter (PSPC) (Rigaku, PSPC-5) with a camera length of 350 mm and associated electronics (e.g., multichannel analyzer; Rigaku) (30–32). In all cases, samples were sealed in a thin-walled glass capillary tube (outer diameter, 1.0 mm) and mounted in a thermostatable holder with a stability of ±0.2°C. The concentration of total phospholipids in the samples used for the SAXS measurements was determined by the Bartlett method.

RESULTS AND DISCUSSION

Induction of calcein leakage from single egg PC-GUVs by EGCg

We first examined the effect of 100 μM EGCg on single egg PC-GUVs containing 1 mM calcein. The EGCg solution in buffer H containing 0.1 M glucose solution was added into the vicinity of an egg PC-GUV via a micropipette controlled by a micromanipulator at room temperature. Before the addition of the EGCg solution, the GUV had high contrast in a phase contrast microscopic image (Fig. 2 *A*, *1*), due to the difference in concentrations of sucrose and glucose between the inside and the outside of the GUV (i.e., 0.1 M sucrose inside the GUV, and 0.1 M glucose outside the GUV). A fluorescence microscopic image of the same GUV (Fig. 2 *A*, *2*) shows that there is a high concentration of calcein inside the GUV at this time. During the addition of the 100 μM EGCg solution, there was a gradual small reduction in the fluorescence intensity inside the GUV over the first 18.73 s; from 18.77 to 22.20 s, the fluorescence intensity decreased rapidly (Fig. 2 *B*, *solid circle*). After 22.20 s, fluorescence was not detected inside the GUV, and a phase contrast image

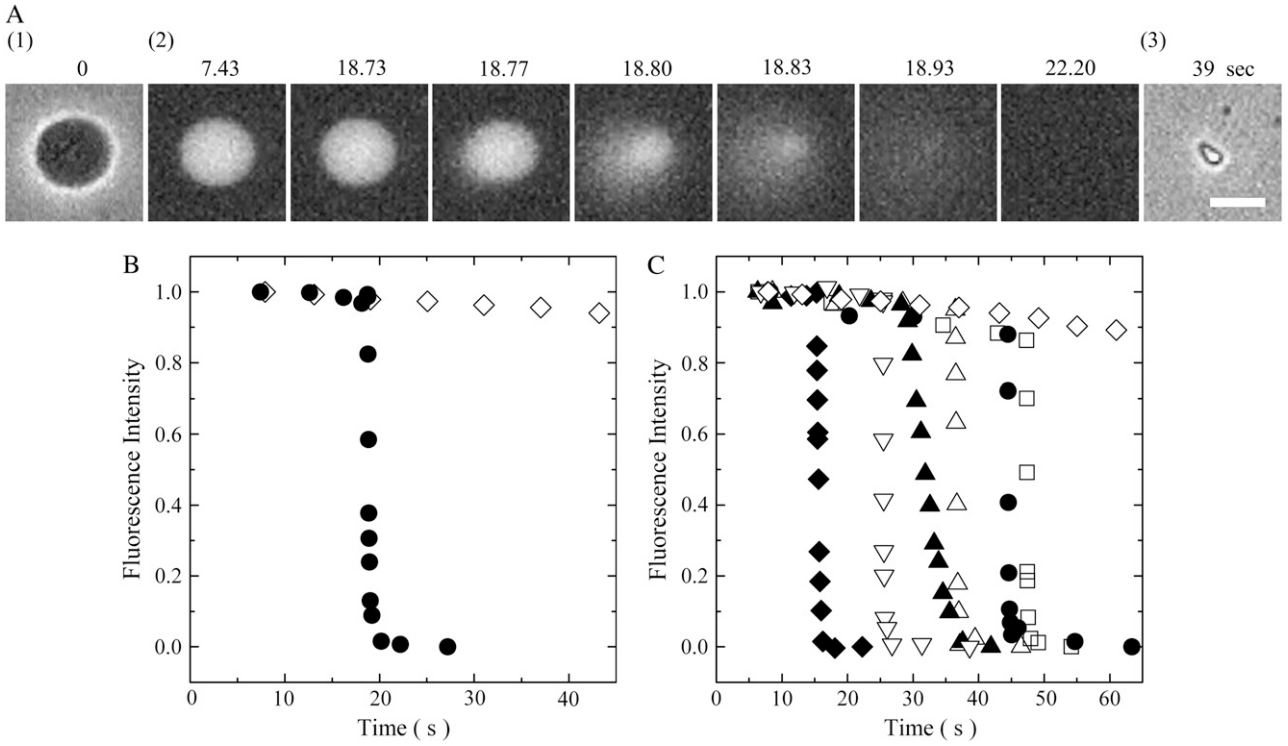

FIGURE 2 Leakage of calcein from single egg PC-GUVs induced by 100 μM EGCg. (*A*) Fluorescence microscope images (2) show that the calcein concentration inside a single GUV progressively decreased after the addition of EGCg. The numbers above each image show the time after the addition of EGCg. Also shown are phase contrast images of the GUV at 0 (1) and at 39 s (3). (*B*) Time course of the change of the fluorescence intensity of the GUV. (●) for the data shown in (*A*) and (◇) for the data of another GUV without the addition of EGCg. (*C*) Other examples of change in the fluorescence intensity of single GUVs with time under the same conditions. Each symbol shows the time course of the change of the fluorescence intensity of each single GUV. The bar corresponds to 10 μm.

of the GUV (Fig. 2 *A*, *3*) showed that the GUV had changed into a small lump of lipid membranes. When we observed single GUVs without the addition of EGCg, as a control experiment, we observed only a continual gradual decrease in the fluorescence intensity with time (Fig. 2 *B*, *diamond*). It suggests that this gradual decrease in the fluorescence intensity was due to the photobleaching of calcein (27). When we examined the interaction of 100 μM EGCg solution with other single egg PC-GUVs using the same method described above, there was a similar rapid complete leakage of calcein from most of the GUVs (Fig. 2 *C*); at first the fluorescence intensity decreased gradually; at $t = t_{tr}$, a rapid decrease in the fluorescence intensity began to occur. Once the fluorescence intensity started to decrease rapidly, it reached zero within 6 $\pm$ 7 s ($n = 15$, where n is the total number of the GUVs, which showed the rapid decrease in the fluorescence intensity in two independent experiments) (e.g., Fig. 2 *C*), as determined by the duration between t_{tr} and the time when the fluorescence intensity, $I(t)$, reached 10% of $I(t_{tr})$. This result indicates that once the leakage of calcein started, all of the calcein molecules leaked from the GUVs within 6 $\pm$ 7 s. After the complete leakage, these single GUVs changed into single small lumps of lipid membranes. Under these conditions, we found that all the leaked GUVs transformed into small lumps of lipid membranes ($n = 15$).

EGCg-induced structural change in single egg PC-GUVs

To elucidate the mechanism of the EGCg-induced leakage of calcein from the GUV, we investigated the process of the transformation of single GUVs into the single small lumps of lipid membranes. Fig. 3 *A* shows a typical example of the 100 μM EGCg-induced transformation of an egg PC-GUV into a small lump. At 27.20 s, many small high-contrast (black) particles appeared on the membrane of the GUV; then, the number of these particles increased and the diameter of the GUV decreased with time. From 27.20 s to 28.50 s, a large hole was observed at the center of the membrane of the GUV. At 30.93 s, the GUV changed into a small lump of lipid membranes. We also observed this process at a higher concentration of EGCg (300 μM) (Fig. 3, *B* and *C*). Fig. 3 *B* more clearly shows a large hole in the membrane of a GUV and shows small high-contrast particles at the edge of the hole. After the large hole appeared, the diameter of the GUV rapidly decreased with time. Fig. 3 *C* shows a side view of the hole formed in the membrane of a

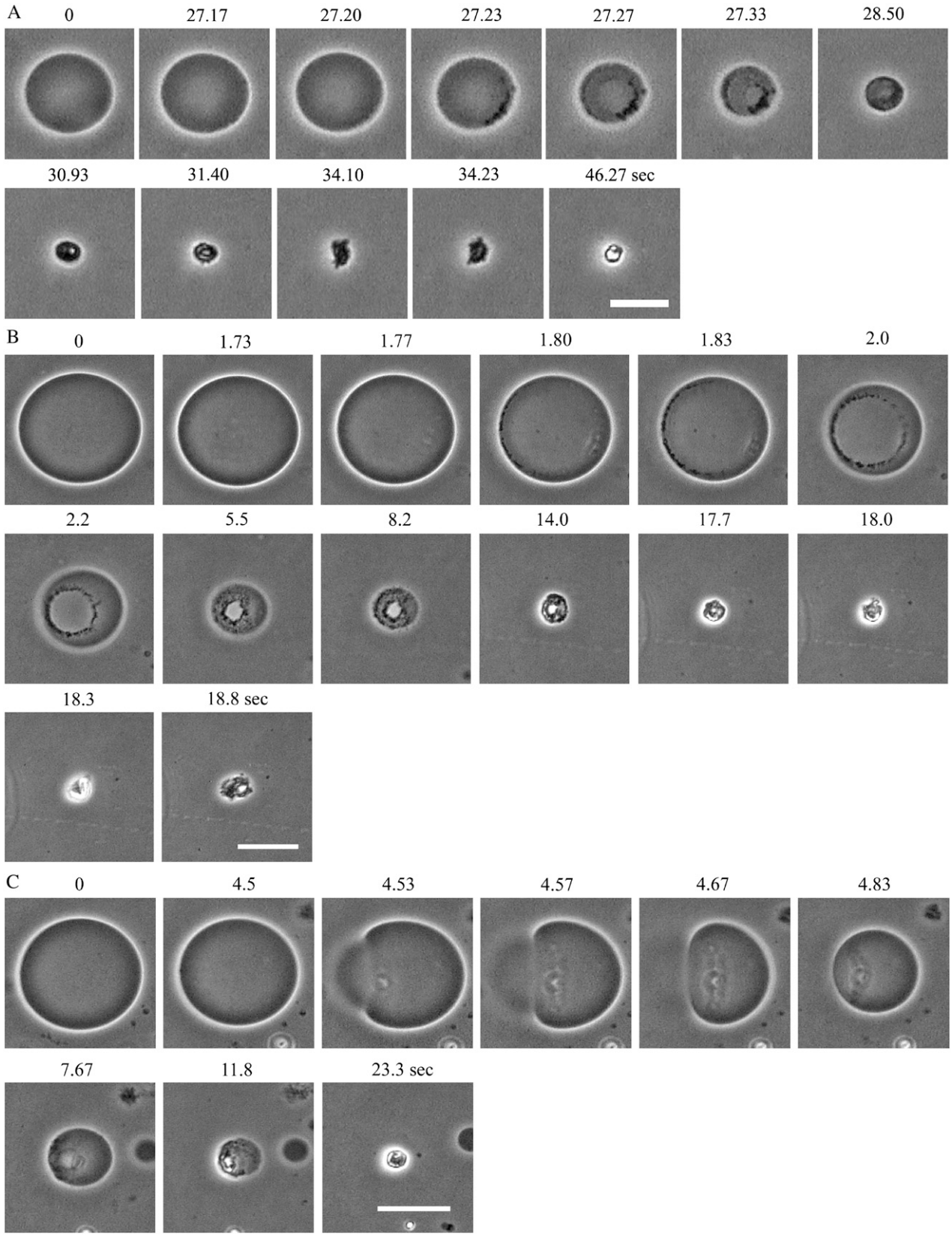

FIGURE 3 Structural change of single egg PC-GUVs induced by EGCg. Phase contrast images of single GUVs in the interaction of (*A*) 100 μM EGCg and (*B*) and (*C*) 300 μM EGCg. The numbers above each image show the time after the addition of EGCg. The bar in (*A*) corresponds to 20 μm, and the bars in (*B*) and (*C*) correspond to 40 μm.

GUV, indicating that sucrose inside the GUV diffused rapidly to the outside of the GUV through the hole. These results show that EGCg induced bursting of the single GUVs without the association of two GUVs. The small lump of lipid membranes may be composed of EGCg and lipid membranes. We discuss its structure and the mechanism of its formation below. The small high-contrast particles observed in the GUV surface comprise complexes of EGCg and PC membranes that are amphipathic, judging from the finding that they appeared at the edge of the hole in the membrane. However, we were unable to determine the exact structure of these particles.

Correlation between calcein leakage from single egg PC-GUVs and EGCg-induced bursting of single egg PC-GUVs

The results here suggest that the leakage of calcein from the inside to the outside of single GUVs occurred as a result of the bursting of the GUVs. To confirm the correlation between the leakage of calcein and the bursting of GUVs, we investigated the effect of EGCg concentration on these phenomena. At 300 μM EGCg, complete leakage of calcein from single GUVs occurred in all the examined single GUVs within 5 min after the addition of EGCg. At a concentration of $\leq$200 μM, EGCg induced the complete leakage of calcein in some, but not all, of the examined GUVs within 5 min, and in other GUVs no leakage occurred. At a very low concentration (10 μM), we did not observe a rapid decrease in the fluorescence intensity, indicating that this concentration of EGCg did not induce the leakage of calcein. These results indicate that, in the estimation of the leakage of the internal contents of a single liposome, an important factor is the probability, $P_L(t)$, that a given liposome (in this case, a GUV) does not contain calcein molecules at any given time, t. Such empty liposomes are produced by the complete leakage of calcein from the liposome at any time within t. Thereby, we call $P_L(t)$ the fraction of completely leaked GUV at t; more concisely, we call it the fraction of leaked GUV. This situation is exactly the same as that of magainin 2-induced leakage from GUVs (27). Fig. 4 *A* (*open square*) shows the dependence of P_L (5 min) on the EGCg concentration. $P_L(t)$ increased as the EGCg concentration increased; at $t = 5$ min, EGCg at a concentration of <30 μM did not induce leakage (i.e., $P_L(5\text{ min}) = 0$), and $P_L(5\text{ min})$ at 30 μM, 50 μM, and 100 μM were 0.07 $\pm$ 0.04, 0.17 $\pm$ 0.06, and 0.79 $\pm$ 0.04 (estimated by three independent experiments), respectively.

On the other hand, in the estimation of the bursting of a single liposome, an important factor is the probability, $P_B(t)$, that a given liposome (in this case, a GUV) is burst at any given time, t. Such burst liposomes are produced by the complete bursting of the liposome at any time within t. Thereby, we call $P_B(t)$ the fraction of burst GUV at t. Fig. 4 *A* also shows the dependence of the fraction of burst GUV, $P_B(t)$, at 5 min on EGCg concentration (*solid circle* in Fig. 4 *A*). In this experiment, we prepared GUVs without calcein solution, and thereby we could not detect its leakage. At a concentration of $\leq$20 μM EGCg, we did not observe the bursting of GUV within 5 min, and at a concentration of $\geq$30 μM EGCg complete bursting was induced in some, but not all, of the examined GUVs within 5 min. $P_B(t)$ increased as the EGCg concentration increased; P_B (5 min) at 30 μM, 50 μM, and 100 μM were 0.19 $\pm$ 0.06, 0.29 $\pm$ 0.16, and 0.96 $\pm$ 0.04 (estimated by three independent experiments), respectively. Fig. 4 *A* indicates that the dependence of the fraction of burst GUV on EGCg concentration (*solid circle* in Fig. 4 *A*) was almost the same as the dependence of the fraction of completely leaked GUV on EGCg concentration (*open square* in Fig. 4 *A*) (i.e., $P_B(t) = P_L(t)$). This correlation strongly indicates that the leakage of calcein from the

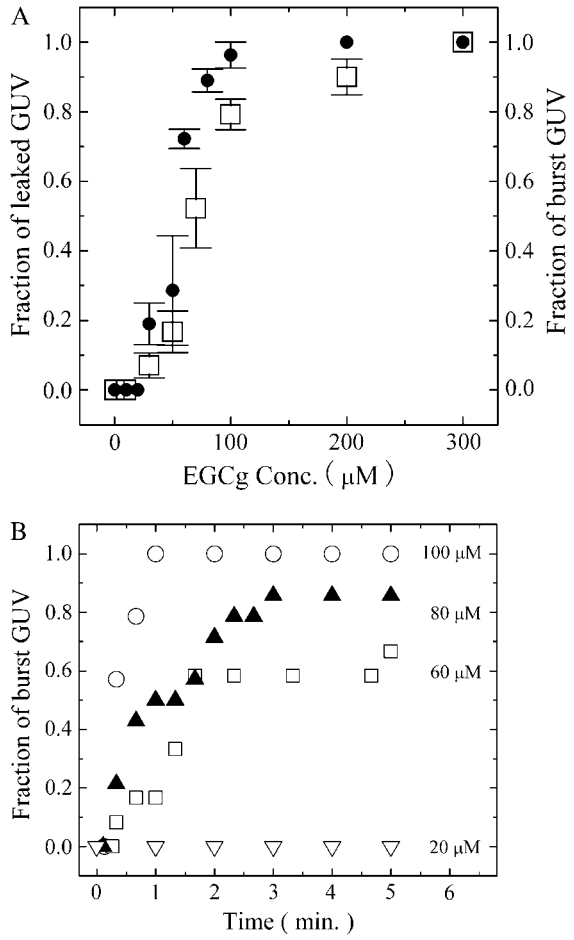

FIGURE 4 (*A*) Dose response of EGCg for the fraction of completely leaked GUV, $P_L(t)$, (□), and for the fraction of burst GUV, $P_B(t)$, (●) among all the examined single egg PC-GUVs at $t = 5$ min after the addition of EGCg. The bars show the standard deviation. The average values of $P_L(t)$ and $P_B(t)$ and their standard deviations were obtained by three independent experiments. (*B*) Time course of the fraction of burst GUV among all the examined single GUVs after the addition of various concentrations of EGCg. (▽) 20 μM, (□) 60 μM, (▲) 80 μM, and (○) 100 μM EGCg.

inside to the outside of the GUV occurred as a result of the bursting of the GUV.

We investigated the time course of the EGCg-induced burst of GUVs using various concentrations of EGCg. Fig. 4 *B* shows that the fraction of burst GUV, $P_B(t)$, increased with time at a concentration of $\geq$30 μM EGCg. The results shown in Fig. 4 *A* suggest that the time course of the fraction of leaked GUV, $P_L(t)$, was almost the same as the time course of the fraction of burst GUV, $P_B(t)$, shown in Fig. 4 *B*.

Comparison between the EGCg-induced calcein leakage from the suspension of egg PC-LUVs and that from single egg PC-GUVs

We next compared the characteristics of EGCg-induced calcein leakage from single GUVs with those of EGCg-induced calcein leakage from many LUVs. Fig. 5 *A* shows the time course of calcein leakage from the egg PC-LUV suspension induced by various concentrations of EGCg. The leakage from these LUVs occurred gradually over a period of 15 min, and the rate of leakage depended on the EGCg concentration. Fig. 5 *B* shows the dependence of the fraction of leakage of calcein from egg PC-LUVs on EGCg concentration at 10 min after mixing the LUV suspension with the EGCg solution. At a concentration of $\geq$50 μM EGCg, leakage of the internal contents of the LUVs occurred, and the amount of the leakage increased with increasing EGCg concentration. These results resemble those obtained in previous leakage studies using LUV suspensions (8,9); the leakage from many LUVs in the suspension increased gradually with time. It has previously been thought that the EGCg-induced leakage of calcein from an ensemble of LUVs occurs gradually from each LUV for 5–15 min; i.e., it takes a long time (5−15 min) for all calcein molecules to leak from each LUV after the leakage starts (8,9). However, the results here using the single GUV method indicate that the complete leakage from single GUVs occurred within a time period below 20 s (Fig. 2 *C*) and that $P_L(t)$ increased with time. These findings indicate that the rate-determining step of the leakage is the bursting of liposomes, rather than the leakage of the internal contents from each liposome, and that the gradual increase in the leakage from an ensemble of LUVs with time (Fig. 5 *A*) is due to the increase in $P_L(t)$ and is therefore due to an increase in the number of individual LUVs that had completely lost their internal contents (i.e., calcein). The threshold EGCg concentration of the leakage from the LUV suspension (50 μM) was almost the same as that of leakage from the single GUVs (70 μM), defined as the concentration at which the leakage occurred in 50% of examined GUVs. This is almost the same as the relationship between the magainin 2-induced leakage of calcein from the ensemble of LUVs and the magainin 2-induced leakage of calcein from single GUVs (27).

However, there is one large difference between the curve of leakage from the LUV suspension (Fig. 5 *A*) and the curve

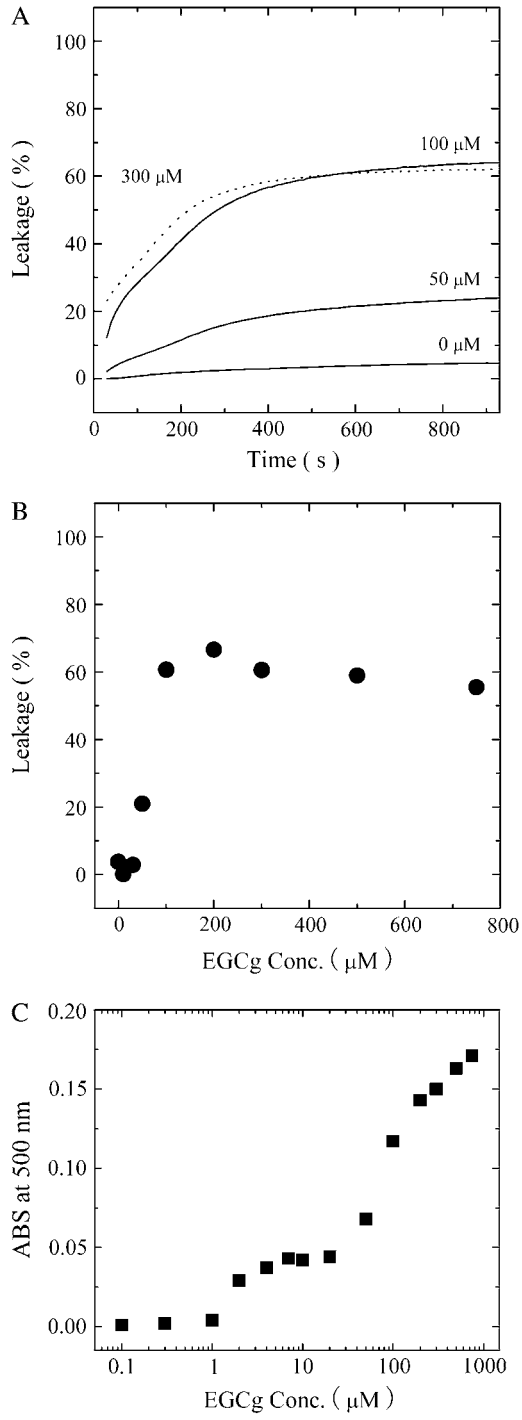

FIGURE 5 (*A*) Time course of EGCg-induced leakage of calcein from a suspension of egg PC-LUVs after the addition of various concentrations of EGCg. (*B*) Dose response of EGCg-induced leakage from a suspension of egg PC-LUVs at 10 min after the addition of EGCg. (*C*) Absorbance change (Abs. at 500 nm) of a suspension of egg PC-LUVs at 10 min after the addition of various concentrations of EGCg.

of the fraction of burst GUV (Fig. 4 *B*), which is almost the same as the curve of the fraction of leaked GUV: the maximum leakage from the LUV suspension was much smaller than the maximum leakage from single GUVs (e.g., at 300 μM EGCg, the former was 61% at 15 min and the latter was 100% at 1 min). We propose the following explanation for this discrepancy. The light scattering intensity of the egg PC-LUV suspension increased with an increase in EGCg concentration (Fig. 5 *C*), suggesting that the association of egg-PC LUVs was induced by EGCg. At a concentration of $\geq$2 μM EGCg, association of the LUVs occurred. At a concentration of $\geq$50 μM EGCg, the light scattering intensity greatly increased (Fig. 5 *C*), and the leakage also occurred at these concentrations of EGCg (Fig. 5 *B*). These results suggest that after the EGCg induced bursting of the LUVs, they transformed into small lumps of lipid membranes, producing the strong light scattering. This result suggests that the association of LUVs may prevent complete leakage from the suspension of LUVs. To confirm this hypothesis, we investigated the effect of EGCg on the interaction of two egg PC-GUVs. When we added 10 μM EGCg solution from the micropipette into the vicinity of two GUVs, a strong association between the two GUVs occurred (Fig. 6 *A*). The binding of EGCg in the membrane interface

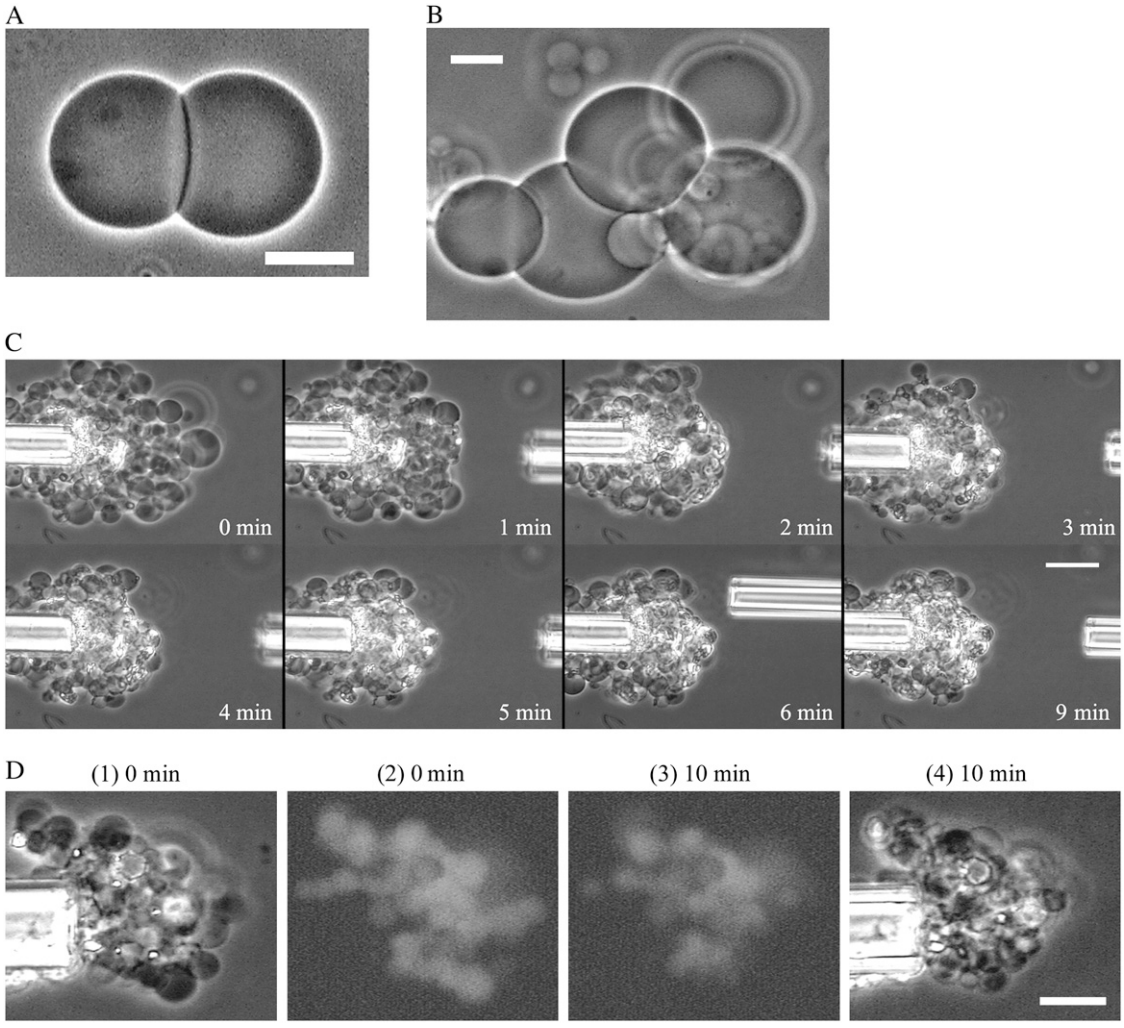

FIGURE 6 (*A*) Phase contrast image of association of two egg PC-GUVs in the presence of 10 μM EGCg. (*B*) Phase contrast image of association of several egg-PC GUVs in the presence of 10 μM EGCg. (*C*) Effect of 100 μM EGCg on the associated egg PC-GUVs. Phase contrast images. At first many egg PC-GUVs were associated around the left micropipette in the presence of 10 μM EGCg, and then we added 100 μM EGCg into the vicinity of the associated GUVs through the right micropipette. GUVs located at the right side of the associated GUVs were burst one by one by the interaction of 100 μM EGCg. The numbers in each image show the time after the addition of EGCg. (*D*) Effect of 500 μM EGCg on the leakage of the associated egg PC-GUVs containing calcein. Phase contrast images (1)(4) and fluorescence microscope images (2)(3). At first many egg PC-GUVs were associated around the left micropipette in the presence of 10 μM EGCg, and then we added 500 μM EGCg into the vicinity of the associated GUVs through the right micropipette (not shown). After the interaction of 500 μM EGCg, high intensity of fluorescence was observed inside the associated GUVs, indicating that many GUVs inside the associated GUVs did not burst and no leakage of the internal content occurred from these GUVs. The numbers above each image show the time after the addition of EGCg. The bars in (*A*), (*B*), and (*D*) correspond to 20 μm, and the bar in (*C*) corresponds to 40 μm.

induces a decrease in the repulsive undulation force of lipid membranes and at the same time a strong attractive force (perhaps due to van der Waals interaction) between the EGCg-bound membranes of the two GUVs; consequently, the two GUVs strongly associate with each other (for details, see the section ''Interaction of EGCg with DOPC-MLV'').

The threshold concentration of EGCg for the induction of the association of two GUVs was 0.6 μM, which was almost the same as that of the association of LUVs (2 μM) and was much lower than that of the bursting of GUVs (55 μM EGCg), defined as the concentration at which the bursting occurred in 50% of examined GUVs. Several GUVs aggregated with each other readily in the presence of EGCg (Fig. 6 *B*). To elucidate the effect of the association of vesicles on the efficiency of the leakage, after many GUVs had associated in the presence of 10 μM EGCg, we added 100 μM EGCg into the vicinity of the associated GUVs from the right micropipette (Fig. 6 *C*). GUVs located on the right side of the associated GUVs in Fig. 6 *C*, which were the first to come in contact with the EGCg solution, burst one by one as they interacted with the 100 μM EGCg. Then, all GUVs at the edge of the associated GUVs burst, but many GUVs inside the associated GUVs did not burst after 9 min of exposure to the EGCg solution (Fig. 6 *C*). We performed similar experiments using egg PC-GUVs containing 1 mM calcein. After the addition of 500 μM EGCg, high-intensity fluorescence was observed inside the associated GUVs (Fig. 6 *D*), indicating that many GUVs inside the associated GUVs did not burst and that no leakage of the internal contents of these GUVs occurred. We conclude that the small lumps of lipid membranes that formed at the edge of the associated GUVs due to the EGCg-induced bursting of GUVs became a kind of wall at the edge, which prevented the EGCg solution from entering the internal region of the associated GUVs. This is one of the main reasons for the low maximum value of the leakage from the LUV suspension. In the LUV suspension, EGCg first induced the association of many LUVs, and then LUVs located at the edge of the associated LUVs burst to form a kind of wall preventing contact between the EGCg solution and the LUVs located in the internal region of the associated LUVs. Thereby, leakage from these LUVs did not occur, causing a decrease in the maximum amount of EGCg-induced leakage.

Shape changes of egg PC-GUVs induced by EGCg

We performed several experiments to clarify the mechanism of the EGCg-induced bursting of GUVs. Analysis of shape changes of GUVs is a highly sensitive method for detecting the interaction of substances with lipid membrane (19,20). For these experiments, we used nonspherical GUVs, because the shape of spherical GUVs cannot be changed when they exist without interaction with other GUVs. The shape of GUVs is determined by the minimization of the elastic energy of the closed membrane, and therefore it depends on several of the conditions existing when these GUVs are formed (see below for details).

To elucidate how EGCg interacts with the egg PC membranes, we investigated its effect on the shapes of egg PC-GUVs. Fig. 7, *A* and *B*, shows two kinds of shape changes in egg PC-GUVs after the addition of low concentrations (5 and 1 μM, respectively) of EGCg into the vicinity of an egg PC-GUV via a micropipette. In the absence of EGCg, the GUV had a prolate shape (Fig. 7 *A*, *1*)). After the addition of 5 μM

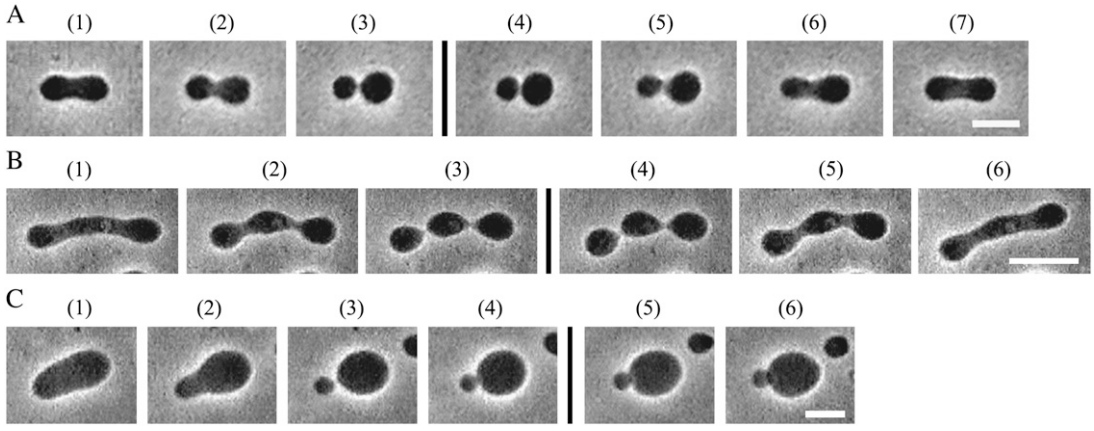

FIGURE 7 Shape changes of egg PC-GUVs induced by the addition of EGCg at room temperature. (*A*) A prolate changed into a dumbbell, and then into two spheres connected by a narrow neck upon addition of 5 μM EGCg. The time after starting addition of EGCg solution through the micropipette is (*1*) 0 s, (*2*) 11 s, and (*3*) 14 s. After the addition of EGCg was stopped, the shape change was reversed. The time after stopping the addition of EGCg is (*4*) 3 s, (*5*) 8 s, (*6*) 11 s, and (*7*) 17 s. (*B*) A cylinder changed into a pearls-on-a-string upon addition of 1 μM EGCg. The time after starting addition of 1 μM EGCg solution through the micropipette is (*1*) 0 s, (*2*) 10 s, and (*3*) 18 s. After the addition of EGCg was stopped, the shape change was reversed. The time after stopping the addition of EGCg is (*4*) 2 s, (*5*) 15 s, and (*6*) 94 s. (*C*) A prolate changed into two spheres connected by a neck upon addition of 1 μM EGCg, and then the two spheres associated each other (*4*). The time after starting addition of 1 μM EGCg solution through the micropipette is (*1*) 0 s, (*2*) 11 s, (*3*) 18 s, and (*4*) 21 s. When EGCg was no longer added, the two associated spheres did not detach. The time after stopping the addition of EGCg is (*5*) 30 s and (*6*) 88 s. The bars in (*A*) and (*C*) correspond to 10 μm, and the bar in (*B*) corresponds to 10 μm.

EGCg, the GUV changed into a dumbbell shape (Fig. 7 *A*, *2*) and then changed into the shape of two spheres connected by a neck (Fig. 7 *A*, *3*). We observed this shape change in eight GUVs among eight examined GUVs ($N = 8$). To determine the reversibility of the shape change, the addition of EGCg was stopped after the complete shape change of the GUV, followed by observation of the shape of the GUV. Fig. 7 *A*, *4–7*) shows the time course of the shape change of the GUV when the addition of EGCg was stopped. First, the two spheres connected by a narrow neck changed into a dumbbell shape (Fig. 7 *A*, *6*), then, the dumbbell shape changed into a prolate shape (Fig. 7 *A*, *7*). When the addition of EGCg was stopped, the EGCg diffused away from the vicinity of the GUV into the bulk solution, inducing a decrease in the EGCg concentration near the GUV, and then the partition of EGCg into the membrane decreased (i.e., EGCg molecules in the external monolayer of the GUV transferred into the aqueous solution). This result indicates that the shape change induced in egg PC-GUV by 5 μM EGCg was reversible. The threshold concentration of EGCg for the shape change (i.e., the EGCg concentration at which the shape change occurred in 50% of examined GUVs) was 0.5 μM. This kind of shape change was not observed when 0.05 μM EGCg was added. Fig. 7 *B* shows another type of shape change: a cylindrical GUV (Fig. 7 *B*, *1*) changed into a series of many smaller spherical vesicles connected by a narrow tube (so-called ''pearls-on-a-string'') (Fig. 7 *B*, *3*) ($N = 5$). To determine the reversibility of the shape change, the addition of EGCg was stopped after the complete shape change of the GUV, followed by observation of the shape of the GUV (Fig. 7 *B*, *4–6*). This shape change was reversible. Again, the threshold concentration of EGCg for the shape change was 0.5 μM, and this shape change was not observed when 0.05 μM EGCg was added.

The results in Fig. 7 clearly show that very low concentrations of EGCg (much less than the threshold concentration of the bursting of GUV) induced shape changes in the egg PC-GUVs. What is the mechanism for these shape changes? The shape of GUV made of lipid membranes is determined by the minimization of the elastic energy of the closed membrane. It is thought that the ''area-difference-elasticity'' model (ADE model), also known as the ''generalized bilayer-couple'' model, reasonably explains such shape changes in GUVs (19,23,33,34). In the ADE model, the area of each monolayer is not fixed to the equilibrium area, but the monolayer membrane can stretch elastically to increase the membrane's nonlocal elastic energy. Thus, the elastic energy of the GUV (W_{el}) can be expressed as a sum of the membrane bending energy and the energy of the relative monolayer stretching. In the ADE model, the shape of the GUV is determined by the minimization of the membrane elastic energy (W_{el}) for a given area A, volume V, and difference ($\Delta A_0 (= A_0^{ex} - A_0^{in})$) between the area of the external (A_0^{ex}) and internal (A_0^{in}) monolayers in the GUV bilayer membrane under the relaxed (i.e., nonstretched) condition (33,34). The analysis based on the ADE model shows that, under the condition of constant volume of the GUV, the shape changes as follows: as ΔA_0 increases, 1), prolate $\rightarrow$ pear (i.e., asymmetric prolate) or dumbbell (i.e., symmetric prolate) $\rightarrow$ two spheres connected by a narrow neck, and 2), cylinder $\rightarrow$ pearls-on-a-string. These shape changes are the same as those induced by EGCg in the egg PC-GUVs (Fig. 7). This analysis therefore shows that EGCg binds to the membrane interface of the external monolayer of the GUVs from the outside aqueous solution, increasing the ΔA_0 of the GUVs. These findings suggest that the reversibility of the EGCg-induced shape change indicates that the binding of EGCg to the membrane interface is also reversible.

We often observed the association of membranes of vesicles during the EGCg-induced shape changes in egg PC-GUV. Fig. 7 *C* shows that after the shape change from prolate (Fig. 7 *C*, *1*) to two spheres connected by a neck (Fig. 7 *C*, *3*), the two spheres associated with each other (Fig. 7 *C*, *4*). When the addition of EGCg was stopped, these two spheres did not detach (Fig. 7 *C*, *5* and *6*). The mechanism of the association of the two spheres in this case is almost the same as the association of two independent GUVs (shown in Fig. 6 *A*). The binding of EGCg in the membrane interface induces a decrease in the repulsive undulation force of lipid membranes and at the same time a strong attractive force (perhaps due to van der Waals interaction) between the EGCg-bound membranes of the two GUVs; consequently, the two GUVs strongly associate with each other (for details, see the section ''Interaction of EGCg with DOPC-MLV''). This result suggests that the association of membranes (or vesicles) prevents the detachment of the EGCg from the membrane interface. It would increase the apparent value of the partition coefficient of EGCg from the aqueous solution to the membrane, which is discussed below.

The mechanism of the binding of EGCg to lipid membranes is unclear. As indicated by the binding of tannic acid, a polyphenol, with lipid membranes (35), the interaction between the electron-rich π system of polyphenol and the $-N^+(CH_3)_3$ group may play an important role in the binding of EGCg to the lipid membranes. However, there is another possible mechanism. Recent biophysical studies indicate that the lipid membrane interface in the L_α phase is composed of hydrophilic segments (so-called headgroups), hydrophobic acyl chains, and water molecules incorporated as a result of large thermal motions of membranes such as undulation and protrusion. Thus, aromatic amino acid residues such as Trp (W) and Phe (F) with high interfacial hydrophobicity can be partitioned into the membrane interface (36). In a previous report, we clearly showed that a de novo designed peptide (WLFLLKKK) containing a segment with high interfacial hydrophobicity (WLFLL) can bind to the electrically neutral membrane interface of a DOPC membrane and a monoolein membrane, increasing the area of monolayer membranes (20,37). Therefore, EGCg may be partitioned into the membrane interface, owing to its high interfacial hydrophobicity.

The reversibility of the EGCg-induced shape changes (Fig. 7, *A* and *B*) indicates that the rate of the translocation (i.e., flip-flop or transverse diffusion) of EGCg from the external to the internal monolayer was very low, i.e., no significant flip-flop occurred in the timescale of this experiment (30–60 s). This result indicates that the concentration of EGCg in the external monolayer is much larger than that in the internal monolayer in the interaction of EGCg with GUVs. Generally, to determine the translocation rate of substances such as lipids quantitatively, spin-labeled and fluorescence analogs are used in LUVs. However, there are no such analogs for EGCg. Recently, Devaux and his colleague developed a new method to determine the translocation rate of unlabeled ceramides using GUVs (38); the incorporation of the ceramides into the external monolayer of a GUV changed a prolate into a pear, and, by observing the reversibility of this shape change, the translocation rate from the external into the internal monolayer of the GUV was obtained. We tried to use a similar method to obtain the translocation rate of EGCg quantitatively. In the same experiments described for Fig. 7 *A*, we continued to add the EGCg solution for a long time after the GUV shape had changed from the prolate to the two spheres connected by a neck. We expected that the shape might reverse into the prolate as a result of the flip-flop of EGCg from the external into the internal monolayer of the GUV. But the long time addition of EGCg solution always induced the association of membranes of the two spheres connected by a neck as shown in Fig. 7 *C*, and thereby, we could not determine the flip-flop rate from this experiment quantitatively. However, we can conclude that the flip-flop rate was low on the basis of the above discussion.

Irrespective of the binding mechanism, the analysis of the EGCg-induced shape changes indicates that EGCg binds to the membrane interface of the external monolayer of the GUVs and induces an increase in the area of the external monolayer. This kind of binding of EGCg in the membrane interface induces the increase in the surface pressure (27); i.e., the lateral tension of the lipid membrane increases. Studies clearly show that an increase in the lateral tension decreases the undulation force of lipid membranes, inducing the association of vesicles (39,40). The threshold EGCg concentration for the shape change was almost the same as the threshold EGCg concentration for the association of two GUVs (0.6 μM). These findings suggest that one of the important factors in the induction of EGCg-induced association of vesicles such as GUVs and LUVs is the decrease in the undulation force due to the lateral tension resulting from the EGCg binding to the membrane.

Binding of EGCg to egg PC membrane

We determined the amount of EGCg that bound to the lipid membrane using the standard method. The fluorescence intensity of EGCg bound to lipid membranes is much greater than the fluorescence intensity of EGCg in water; thus, the fluorescence intensity of EGCg depends on the lipid concentration in aqueous solution (11). We measured the fluorescence intensity of EGCg in the presence of various concentrations of egg PC-LUVs. The fluorescence intensity of EGCg increased with increasing lipid concentration (Fig. 8). The partition coefficient of EGCg from aqueous solution to lipid membrane, K_p, is defined as follows:

$$\frac{n_L}{V_L} = K_p \frac{n_w}{V_w}, \tag{1}$$

where n_L and n_w are the number of moles of EGCg partitioned in the lipid membrane and the number of moles of EGCg solubilized in the aqueous solution at equilibrium, respectively, and V_L and V_w are the volume (l) of the lipid membrane and aqueous solution, respectively. We can determine the volume of the lipid membrane using the equation $V_L = \gamma[L]\ V_t$, where γ is the molar volume of the lipid membrane (l/mol), [L] is the lipid concentration in the aqueous solution (M), and V_t is the total volume ($= V_L + V_w$). Because the volume fraction of the lipid membrane is very small, we can use an approximate equation ($V_t = V_w$). The molar volume of egg-PC at 20°C, γ, is 0.764 (l/mol) (41).

$$\frac{n_L}{n_w} = 0.764 \times K_p[L]. \tag{2}$$

The difference between the fluorescence intensity of EGCg in the presence of egg PC-LUVs, $F([L])$, and the fluorescence intensity of EGCg in the absence of egg PC-LUVs, $F(0)$, can be determined using the equation $\Delta F([L]) = F([L]) - F(0)$ and can be expressed as a function of [L], as follows (11):

$$\Delta F([L]) = \frac{K_p \gamma[L] \Delta F_{max}}{1 + K_p \gamma[L]}, \tag{3}$$

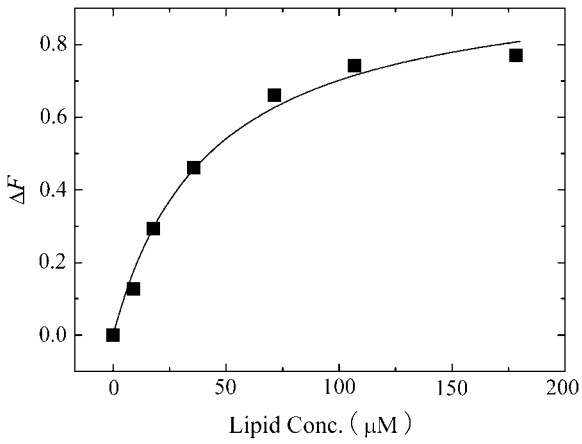

FIGURE 8 Dependence of the difference between the fluorescence intensity of 10 μM EGCg solution in the presence of egg PC-LUVs and that in the absence of egg PC-LUVs on the lipid concentration. The solid line represents a best fitted curve of Eq. 3.

where ΔF_{max} is the limiting value of ΔF when lipid concentration increased. The best fit of the experimental values in Fig. 8 with the theoretical curve (Eq. 3) gave the partition coefficient of EGCg (K_p) as 3.1×10^4. This value is almost the same as those reported as K_p for EGCg with other lipid (dimyristoylphosphatidylcholine (DMPC)) membranes in the L_α phase (11). Therefore, we can determine the ratio of the number of moles of EGCg in the lipid membrane to the number of moles of EGCg in the aqueous solution using the following equation:

$$\frac{n_L}{n_w} = 2.37 \times 10^4 \times [L]. \quad (4)$$

Using Eq. 1, we can determine the molar ratio, X_b, of the EGCg bound to (or partitioned into) the lipid membrane, n_L, to the lipid in the external monolayer of vesicles such as GUVs and LUVs, [L] $V_t/2$, as a function of free (i.e., not bound) EGCg concentration in the aqueous solution, C_w ($= n_w/V_w$) (M), as follows:

$$X_b = \frac{n_L}{[L]V_t/2} = 2\gamma K_p C_w = 4.74 \times 10^4 \times C_w. \quad (5)$$

The advantage of the single GUV method over the conventional LUV suspension method is that we can accurately control the concentration of test substances in the aqueous solution near a vesicle, which is the same as that of the solution introduced by the micropipette (19,20,22,23,27). In the LUV suspensions, the free (equilibrium) concentration of the test substance in the aqueous solution is smaller than the concentration of the test substance in the absence of LUVs and decreases with increasing lipid concentration as a result of the binding of the test substance to the LUV membranes (42). As described above, the threshold concentration of EGCg for the induction of the bursting of GUVs was 55 μM EGCg. We can obtain X_b under this condition using Eq. 5: $X_b = 2.8$ for $C_w = 60 \times 10^{-6}$ M. This gives an unexpectedly high value for the molar ratio: 2.8 molecules of EGCg are bound to lipid membrane per lipid molecule. We conclude that the K_p value determined from the fluorescence intensity of the LUV suspension was overestimated because the association of LUVs was accompanied by the binding of EGCg to the lipid membrane interface, and EGCg molecules located in the associated membrane sites cannot detach easily from the membrane interface, possibly resulting in the stronger binding of EGCg to the membrane (i.e., increased apparent partition coefficient, K_p). The results shown in Fig. 7 *C* support this hypothesis. Moreover, there is a possibility that the partition coefficient, K_p, depends on the curvature of membranes; K_p for GUV membranes may be smaller than that for LUV membranes, which can also explain the estimated high binding of EGCg to the GUV membranes. To obtain a more accurate value for the partition coefficient, we need to develop a new method to determine the partition coefficient of test substances using the single GUV method.

Interaction of EGCg with DOPC-MLV

DOPC-MLV in excess water at 20°C is in the liquid-crystalline (L_α) phase (19). We investigated the dependence of spacing of the DOPC-MLV on the EGCg concentration using SAXS. First, we used 10.8 mM DOPC-MLV as the final lipid concentration. For DOPC-MLV in buffer H in the absence of EGCg, a set of SAXS peaks appeared with a spacing ($d_l = 6.0$ nm) at a ratio of 1:2 (Fig. 9 *A*), which is consistent with the L_α phase. On the other hand, for DOPC-MLV in the presence of 6 mM EGCg, a set of SAXS peaks appeared with a short spacing ($d_l = 5.1$ nm) at a ratio of 1:2 (Fig. 9 *B*), indicating that it was in the L_α phase with a short spacing. We investigated a detailed dependence of the spacing of DOPC-MLV on EGCg concentration (Fig. 9 *C*). At a low concentration of EGCg (below 3.5 mM), the spacing of DOPC-MLV decreased with increasing EGCg concentration. At a concentration of ≥3.5 mM EGCg, the spacing nearly remained constant (5.1 nm). The spacing is determined by the summation of the intermembrane distance (d_f) and the membrane thickness (d_m): $d_l = d_f + d_m$. The values of d_f and d_m can be determined from the electron density profile of membranes (30). However, in the presence of EGCg only two diffraction peaks were obtained; thus, it was difficult to obtain the electron density profile. Despite this result, we can obtain qualitative information about the intermembrane distance (d_f) from Fig. 9 *C*. The membrane thickness of the L_α-phase membrane cannot change greatly (20,37). Therefore, the large decrease in the spacing of DOPC-MLV is due to the decrease in the intermembrane distance.

We also investigated the effect of EGCg concentration on the spacing of DOPC-MLV at different concentrations of lipids (Fig. 9 *D*). For 5.4 mM DOPC-MLV, at a low concentration of EGCg (below 2.0 mM), the spacing of DOPC-MLV decreased with increasing EGCg concentration, and at a concentration of ≥2.0 mM EGCg the spacing nearly remained constant (5.2 nm). For 54 mM DOPC-MLV, at a concentration of ≥20 mM EGCg, the spacing nearly remained constant (4.8 nm). However, at a low concentration of EGCg (below 20 mM), only broad peaks were observed, which could not be analyzed, probably because it was difficult to attain the equilibrium state in the complex of EGCg and DOPC membranes. We plotted the relationship between the spacing and the EGCg/lipid molar ratio, e.g., [EGCg]/[lipid] (Fig. 9 *D*). At and above the critical ratio [EGCg]/[lipid] = 0.32–0.37, the spacing nearly remained constant (4.8~5.2 nm). Nagle and Tristram-Nagle (43) estimated the membrane thickness of a DOPC membrane in excess water as 4.5 nm by performing an elaborate analysis. These findings suggest that the intermembrane distance of the DOPC-MLV was very small at and above the critical EGCg concentration. This strongly suggests that the neighboring membranes are in close contact with each other, which is the same situation as in the interaction of negatively charged lipid membranes with positively charged poly(L-lysine) (44). We

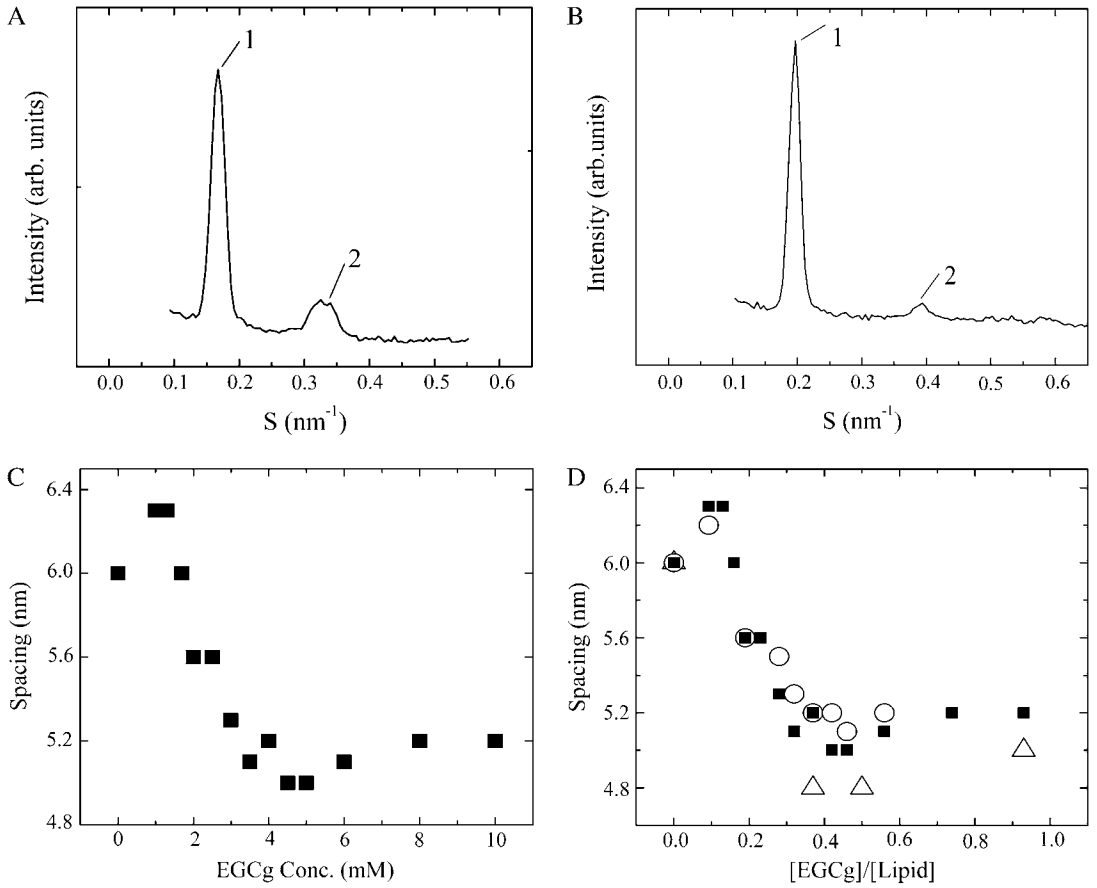

FIGURE 9 SAXS patterns of DOPC-MLV in the absence of EGCg (*A*) and in the presence of 6 mM EGCg (*B*) in buffer H at 25°C. (*C*) Dependence of the spacing of DOPC-MLV on EGCg concentration. For (*A*)–(*C*), final lipid concentration and the total solution volume before the centrifugation were 10.8 mM and 1.0 ml, respectively. (*D*) Dependence of the spacing of DOPC-MLV on the EGCg/lipid molar ratio, [EGCg]/[lipid]. (○) 5.4 mM, (■) 10.8 mM, and (△) 54 mM final lipid concentrations.

consider the mechanism of the association between two bilayers as follows. As described above, the binding of EGCg in the membrane interface induces the increase in the surface pressure, which induces the decrease in the undulation force of lipid membranes. This decreases the repulsive intermembrane force between the neighboring two bilayers in the DOPC-MLV, and thereby, the intermembrane distance decreased with increasing EGCg concentration (Fig. 9 *C*). At and above EGCg concentration, the repulsive undulation force becomes very small and at the same time a strong attractive force (perhaps due to van der Waals interaction) between the EGCg-bound bilayers arises; consequently, the bilayers bound to EGCg molecules strongly associate with each other.

Using the partition coefficient K_P and Eq. 2, we can calculate the free EGCg concentration in aqueous solution at and above the critical concentration of EGCg. For example, for 10.8 mM DOPC-MLV and $V_t = 1.0$ ml, the critical concentration of EGCg was 3.5 mM, where the free EGCg concentration in the aqueous solution was 14 μM. For 5.4 mM and 54 mM DOPC-MLVs, we obtained similar results. This EGCg concentration is less than the threshold EGCg concentration for induction of the bursting of egg PC-GUVs (55 μM). These findings suggest that after the bursting of GUVs, the membranes associate with each other via the same mechanism involved in the EGCg-induced association of the neighboring membranes in DOPC-MLVs, which induces the formation of small lumps.

Mechanism of the EGCg-induced burst of GUVs

We propose a hypothesis for the mechanism of the EGCg-induced bursting of GUVs. First, EGCg binds to the membrane interface of the external monolayer of the GUV (B state). At the critical concentration of EGCg, the bursting of GUVs occurs, and then the membrane of the GUVs transforms into the above-described small lumps. The rate constant of transition from the B state to the bursting of the GUV, k_P, depends on activation energy (energy barrier), E_P, and is given by the following equation:

$$k_P = A\exp(-E_P/k_BT), \quad (6)$$

where k_B is Boltzmann's constant and T is absolute temperature. However, individual events of the transition occur stochastically, as is well demonstrated by force-induced unfolding of proteins (45) and magainin 2-induced pore formation in GUVs (27). To estimate the rate constant, k_P, we must obtain the fraction of GUVs that is in the B state, which can be determined from the fraction of intact GUVs which did not burst (i.e., the fraction of intact GUVs), designated as $P_{intact}(t)$. We obtained $P_B(t)$ as a function of time (Fig. 4 *B*); therefore, we can determine $P_{intact}(t)$ from the equation $P_{intact}(t) = 1 - P_B(t)$. Fig. 10 shows the time course of the fraction of the B state (i.e., the fraction of intact GUV) in the presence of various concentrations of EGCg. The fraction of the B state can be expressed using the rate constant, k_P, as follows:

$$P_{intact}(t) = \exp(-k_P(t - t_{eq})), \quad (7)$$

where t_{eq} is an adjustable parameter. We do not know the exact time required for the equilibration of the EGCg concentration in the vicinity of a GUV or the time required for the binding equilibrium of EGCg from aqueous solution to the membrane interface of the GUV. We can reasonably consider that t_{eq} is the time when the binding equilibrium of EGCg is attained; thus, the state of the GUV becomes the B state at t_{eq}. All the curves of the time course of the fraction of the B state were well fitted with the single exponential function defined by Eq. 7 (Fig. 10). The rate constant increased with increasing EGCg concentration: k_P for 100 μM EGCg, 2.5 $\pm$ 0.5 min^{-1}; 80 μM EGCg, 1.2 $\pm$ 0.6 min^{-1}; 60 μM EGCg, 0.35 $\pm$ 0.04 min^{-1} (estimated by three independent experiments). These results indicate that the EGCg-induced bursting of the GUV apparently followed the first-order reaction.

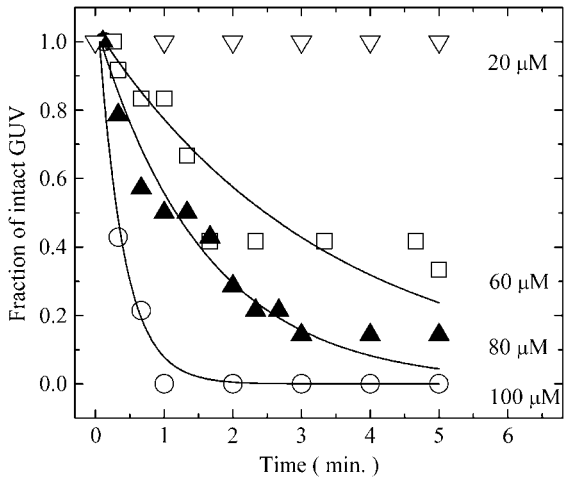

FIGURE 10 Time course of the fraction of intact GUV, $P_{intact}(t)$, after the addition of various concentrations of EGCg. (*C*) (▽) 20 μM, (□) 60 μM, (▲) 80 μM, and (○) 100 μM EGCg. Solid lines represent the best fitted curves of Eq. 7.

Here, we propose a hypothesis of the mechanism of the EGCg-induced bursting of GUVs. Fig. 7 shows that the shape changes in the GUVs were induced at very low concentrations of EGCg, which could not induce the bursting of GUVs. The reversibility of the EGCg-induced shape changes indicates that the rate of the translocation of EGCg from the external to the internal monolayer was very low. Therefore, the nature of these shape changes indicates that the area of the external monolayer of the GUV increases with an increasing amount of the EGCg bound to the external monolayer of the GUV, inducing the increase in the surface pressure of the external monolayer. As the amount of the bound EGCg in the external monolayer increases, the free energy of the B state increases, causing a decrease in the activation energy, E_p. As a result, the rate constant of the burst of the GUV increases as the EGCg concentration is raised. This hypothesis for the mechanism is consistent with the dependence of k_P on the EGCg concentration observed here (Fig. 4).

In most cases of the EGCg-induced bursting of the GUV here, we observed a large hole in the GUV (Fig. 3). We often observed that a portion of the GUV's membrane was detached from the GUV into the aqueous phase. However, the details of the process from the bursting to the formation of the small lumps of lipid membranes are unclear. As described in the previous section, at the EGCg concentration that induced the bursting of the GUV, lipid membranes can come in close contact with each other due to their interaction with EGCg, which was demonstrated by the SAXS experiments (Fig. 9). These findings suggest that the small lumps formed after the bursting of the GUV may be composed of strongly associated lipid membranes, with the association induced by EGCg.

It was reported that a similar breakage of giant vesicles occurred in a DMPC/melittin (10:1, molar ratio) membrane (46). At a temperature above the chain-melting transition temperature (T_m), giant MLVs of the DMPC/melittin membrane were formed and were stable. As the temperature was decreased, at a temperature close to the T_m, many small pores were formed in the surface of the vesicles, and at a temperature below the T_m, the vesicles were broken and no smaller vesicles were observed. On the basis of much experimental data, the authors proposed a mechanism as follows. At a temperature close to the T_m, a large number of melittin molecules associate with each other by facing the hydrophilic side together to form the pore in the membrane (in this case, the hydrophobic side of melittin faces the hydrophobic core of the lipid membrane), that is, the melittin molecules form a barrel-stave type pore. At a temperature below the T_m, the giant MLVs transformed into many small discoidal lipid bilayers which were surrounded by the belt of melittin. In contrast, we conclude that the small lump formed after the EGCg-induced bursting of the GUV may be a multilayer membrane composed of strongly associated lipid membranes, with the association induced by EGCg, which is

completely different from the melittin-induced discoidal membrane. Moreover, in the talin (a cytoskeletal submembranous protein)-induced formation of a large hole in a GUV, talin accumulated along the free verge of the large holes, and the pore formation was reversible, i.e., the dilution of talin reversed the morphological changes (17). One of the reasons for the irreversibility of the EGCg-induced pore formation is that strong attractive force between the EGCg-bound membranes rapidly induced the small lump and prevented the detachment of the membranes. In the EGCg-induced large hole in the membrane of a GUV, small high-contrast particles at the edge of the hole were observed (e.g., Fig. 3, *A* and *B*). In this case, the hydrophobic side of EGCg molecules may face the hydrophobic core of the lipid membrane at the hole to stabilize the interaction between the hydrophobic core and water in the hole, which may be a similar mechanism to that of the melittin-induced pore and the talin-induced large hole.

Advantage of the single GUV method

In the field of functional studies of biomembranes and lipid membranes, such as interactions of various substances (e.g., drugs, peptides, and proteins) with lipid membranes and also dynamics of biomembranes and lipid membranes such as membrane fusion and vesicle fission, all studies of liposomes have been conducted using a suspension of many small liposomes, such as SUVs and LUVs, and various physicochemical methods (i.e., the conventional LUV suspension method). In those studies, the average values of the physical parameters of liposomes were obtained from a large number of liposomes, and thereby much information was lost. We have proposed a novel method, the single GUV method, to probe functions and dynamics of biomembranes (21,27). In the single GUV method, we observe structures and physical properties of single GUVs as a function of time and spatial coordinates and make statistical analysis of the physical properties of a single GUV over many single GUVs. Using the single GUV method, we have succeeded in observing individual events in single GUVs, such as the EGCg-induced bursting of GUVs, the pore formation induced by magainin 2 (27), the membrane fusion of two GUVs (22), and the vesicle fission of single GUVs induced by single long chain amphiphiles such as lyso-PC and lysophosphatidic acid (23,47). The single GUV method enabled us, for the first time to our knowledge, to investigate the detailed elementary processes of these events, which have never been revealed by the conventional LUV suspension method. The results in this study as well as our previous one (27) strongly indicated that, in the measurement of leakage of internal contents induced by the interaction of substances with lipid membranes, the single GUV method will give us direct evidence for the cause of the leakage. Moreover, the statistical analysis of individual events in single GUVs over many GUVs gave us important information on the rate constants of elementary processes, such as the rate constant of the EGCg-induced bursting of GUVs and the rate constant of the pore formation induced by magainin 2 (27). One more advantage of the single GUV method, as described above, is the precise control of concentration of substances in a buffer near single GUVs (27). In the case of the LUV suspension method, there is large area of membranes due to many LUVs in the solution, and thereby, the free (equilibrium) concentration of substances in the bulk solution is smaller than that in the absence of LUVs and decreases with an increase in lipid concentration as a result of the binding of the substances to the LUV membranes (42). On the other hand, in the single GUV method, the substance concentration near a single GUV is constant, the same as that of the substance concentration introduced by the micropipette, because a given concentration of substance solution is continually added into the vicinity of the single GUV from the micropipette. However, this method of the addition of a substance solution through a micropipette has a technical drawback: small dilution of the substance solution occurs due to the diffusion of the substance in a buffer, and thereby the substance concentration near the single GUV is a little lower than that of the solution in the micropipette (23). Development of a new technical method to add a substance solution near a single GUV will solve this drawback near future.

CONCLUSION

Using the single GUV method, we clearly showed that low concentrations of EGCg induced the bursting of egg-PC GUVs, resulting in the formation of small lumps of lipid membranes, and that during the bursting, leakage of the internal contents occurred rapidly. The fraction of burst GUVs, and thereby the fraction of completely leaked GUVs, increased with time, which is consistent with the characteristics of the EGCg-induced leakage from egg PC-LUV suspensions. The experimental results on the EGCg-induced association of neighboring membranes of DOPC-MLV and the partition coefficient of EGCg from the aqueous solution to the lipid membrane provide important clues to the mechanism of the formation of the small lumps of lipid membranes. We have proposed a mechanism for the EGCg-induced bursting of egg PC-GUVs based on the analysis of the EGCg-induced shape changes in the GUVs. The novel results obtained using the single GUV method showed completely new aspects of interaction of EGCg with lipid membranes. On the other hand, when we consider the mechanism of the antibacterial activity of EGCg, it is important to consider the main target of EGCg in vivo. Membranes of bacteria are composed of various kinds of lipids and membrane proteins, which may be one of targets of EGCg. Therefore it is difficult to conclude that the EGCg-induced bursting of GUVs is a main mechanism of its antibacterial activity in vivo. However, it is clear that the EGCg has a strong ability for bursting GUVs, and we believe that the EGCg-induced bursting of

GUVs plays an important role in its antibacterial activity. Further careful investigation is necessary. In contrast to bacteria, human cells have an activity to protect the bursting of cells induced by catechins such as EGCg, which has been obtained in their evolution. It is very important to elucidate the mechanism of the protection against the bursting at a next step.

Our results in this study as well as our previous one (27) strongly indicate the advantage of the single GUV method over the conventional LUV suspension method, especially in the measurement of leakage of internal contents induced by the interaction of substances with lipid membranes. We can prepare various kinds of GUVs composed of many kinds of lipids and also various membrane proteins, and thereby in some cases such GUVs are more useful for the single GUV method. We believe that the single GUV method is a powerful method for examining the interaction of various substances such as polyphenols, peptides, and proteins with lipid membranes and reconstituted membranes containing membrane proteins.

We thank Dr. Masum Shah Md. and Mr. Yasuyuki Inaoka for their critical reading and comments and Mr. Yoshihide Okamoto for his technical assistance. This work was partially carried out using an instrument at the Center for Instrumental Analysis of Shizuoka University.

This work was supported in part by a Grant-in-Aid for General Scientific Research (B) (No. 17310071) and by a Grant-in-Aid for Scientific Research in Priority Areas (System Cell Engineering by Multi-scale Manipulation) (No. 18048020) from the Ministry of Education, Science, and Culture (Japan) to M.Y. This work was also supported by a research fellowship from Radiochemical Research Laboratory, Faculty of Science, Shizuoka University to Y.T.

REFERENCES

1. Sakanaka, S., M. Kim, M. Taniguchi, and T. Yamamoto. 1989. Antibacterial substances in Japanese green tea extract against Streptococcus mutans, a cariogenic bacterium. *Agric. Biol. Chem.* 53:2307–2311.
2. Kono, K., I. Tatara, S. Takeda, K. Arakawa, and Y. Hara. 1994. Antibacterial activity of epigallocatechin gallate against methicillin-resistant Staphylococcus aureus. *Kansenshogaku Zasshi.* 68:1518–1522.
3. Mabe, K., M. Yamada, I. Oguni, and T. Takahashi. 1999. In vitro and in vivo activities of tea catechins against Helicobacter pylori. *Antimicrob. Agents Chemother.* 43:1788–1791.
4. Wang, H., G. J. Provan, and K. Helliwell. 2000. Tea flavonoids: their functions, utilization and analysis. *Trends Food Sci. Tech.* 11:152–160.
5. Guo, Q., B. Zhao, M. Li, S. Shen, and W. Xin. 1996. Studies on protective mechanisms of four components of green tea polyphenols against lipid peroxidation in synaptosomes. *Biochim. Biophys. Acta.* 1304:210–222.
6. Yokozawa, T., E. J. Cho, Y. Hara, and K. Kitani. 2000. Antioxidative activity of green tea treated with radical inhibitor 2,2′-azobis(2-amidinopropane) dihydrochloride. *J. Agric. Food Chem.* 48:5068–5073.
7. Yoshioka, H., Y. Ohashi, M. Akaboshi, Y. Senba, and H. Yoshioka. 2001. A novel method of measuring hydroxyl radical-scavenging activity of antioxidants using gamma-irradiation. *Free Radic. Res.* 35: 265–271.
8. Ikigai, H., T. Nakae, Y. Hara, and T. Shimamura. 1993. Bactericidal catechins damage in lipid bilayer. *Biochim. Biophys. Acta.* 1147: 132–136.
9. Kitano, K., K. Y. Nam, S. Kimura, H. Fujiki, and Y. Imanishi. 1997. Sealing effects of (−)-epigallocatechin gallate on protein kinase C and protein phosphatase 2A. *Biophys. Chem.* 65:157–164.
10. Kajiya, K., S. Kumazawa, and T. Nakayama. 2001. Steric effects on interaction of tea catechins with lipid bilayers. *Biosci. Biotechnol. Biochem.* 65:2638–2643.
11. Caturla, N., E. Vera-Samper, J. Villalain, R. Mateo, and V. Micol. 2003. The relationship between the antioxidant and the antibacterial properties of galloylated catechins and the structure of phospholipid model membranes. *Free Rad. Biol. Med.* 34:648–662.
12. Kajiya, K., H. Hojo, M. Suzuki, F. Nanjo, S. Kumazawa, and T. Nakayama. 2004. Relationship between antibacterial activity of (+)-catechin derivatives and their interaction with a model membrane. *J. Agric. Food Chem.* 52:1514–1519.
13. Kumazawa, S., K. Kajiya, A. Naito, H. Saito, S. Tsuji, M. Tanio, M. Suzuki, F. Nanjo, E. Suzuki, and T. Nakayama. 2004. Direct evidence of interaction of a green tea polyphenol, epigallocatechin gallate, with lipid bilayers by solid-state nuclear magnetic resonance. *Biosci. Biotechnol. Biochem.* 68:1743–1747.
14. Yoshioka, H., H. Haga, M. Kubota, Y. Sakai, and H. Yoshioka. 2006. Interaction of (+)-catechin with a lipid bilayer studied by the spin probe method. *Biosci. Biotechnol. Biochem.* 70:395–400.
15. Evans, E., and E. Rawicz. 1990. Entropy-driven tension and bending elasticity in condensed-fluid membranes. *Phys. Rev. Lett.* 64:2094–2097.
16. Farge, E., and P. F. Devaux. 1992. Shape changes of giant liposomes induced by an asymmetric transmembrane distribution of phospholipids. *Biophys. J.* 61:347–357.
17. Saitoh, A., K. Takiguchi, Y. Tanaka, and H. Hotani. 1998. Opening-up of liposomal membranes by talin. *Proc. Natl. Acad. Sci. USA.* 95: 1026–1031.
18. Tsumoto, K., S. Nomura, Y. Nakatani, and K. Yoshikawa. 2001. Giant liposome as a biochemical reactor: transcription of DNA and transportation by laser tweezers. *Langmuir.* 17:7225–7228.
19. Tanaka, T., Y. Tamba, S. M. Masum, Y. Yamashita, and M. Yamazaki. 2002. La^{3+} and Gd^{3+} induce shape change of giant unilamellar vesicles of phosphatidylcholine. *Biochim. Biophys. Acta.* 1564:173–182.
20. Yamashita, Y., S. M. Masum, T. Tanaka, and M. Yamazaki. 2002. Shape changes of giant unilamellar vesicles of phosphatidylcholine induced by a de novo designed peptide interacting with their membrane interface. *Langmuir.* 18:9638–9641.
21. Yamazaki, M., and Y. Tamba. 2005. The single GUV method for probing biomembrane structure and function. *e-J. Surf. Sci. Nanotech.* 3:218–227.
22. Tanaka, T., and M. Yamazaki. 2004. Membrane fusion of giant unilamellar vesicles of neutral phospholipid membranes induced by La^{3+}. *Langmuir.* 20:5160–5164.
23. Tanaka, T., R. Sano, Y. Yamashita, and M. Yamazaki. 2004. Shape changes and vesicle fission of giant unilamellar vesicles of liquid-ordered phase membrane induced by lysophosphatidyl-choline. *Langmuir.* 20: 9526–9534.
24. Yamazaki, M., and T. Ito. 1990. Deformation and instability in membrane structure of phospholipid vesicles caused by osmophobic association: mechanical stress model for the mechanism of poly(ethylene glycol)-induced membrane fusion. *Biochemistry.* 29:1309–1314.
25. Matsuzaki, K., O. Murase, N. Fujii, and K. Miyajima. 1995. Translocation of a channel-forming antimicrobial peptide, magainin 2, across lipid bilayers by forming a pore. *Biochemistry.* 34:6521–6526.
26. Boggs, J. M., J. Euijung, I. V. Polozov, R. F. Epand, G. M. Anantharamaiah, J. Blazyk, and R. M. Epand. 2001. Effect of magainin, class L, and class A amphipathic peptides on fatty acid spin labels in lipid bilayers. *Biochim. Biophys. Acta.* 1511:28–41.
27. Tamba, Y., and M. Yamazaki. 2005. Single giant unilamellar vesicle method reveals effect of antimicrobial peptide magainin 2 on membrane permeability. *Biochemistry.* 44:15823–15833.

28. Yamashita, Y., M. Oka, T. Tanaka, and M. Yamazaki. 2002. A new method for preparation of giant liposomes in high salt concentrations and growth of protein microcrystals in them. *Biochim. Biophys. Acta.* 1561:129–134.

29. Rasband, W. S. 1997–2006. Image J. U.S. National Institutes of Health, Bethesda, MD. http://rsb.info.nih.gov/ij/.

30. Kinoshita, K., S. Furuike, and M. Yamazaki. 1998. Intermembrane distance in multilamellar vesicles of phosphatidylcholine depends on the interaction free energy between solvents and the hydrophilic segments of the membrane surface. *Biophys. Chem.* 74:237–249.

31. Furuike, S., V. G. Levadny, S. J. Li, and M. Yamazaki. 1999. Low pH induces an interdigitated gel to bilayer gel phase transition in dihexadecylphosphatidylcholine membrane. *Biophys. J.* 77:2015–2023.

32. Li, S. J., Y. Yamashita, and M. Yamazaki. 2001. Effect of electrostatic interactions on phase stability of cubic phases of membranes of monoolein/dioleoylphosphatidic acid mixture. *Biophys. J.* 81:983–993.

33. Heinrich, V., S. Svetina, and B. Zeks. 1993. Nonaxisymmetric vesicle shapes in a generalized bilayer-couple model and the transition between oblate and prolate axisymmetric shapes. *Phys. Rev. E.* 48:3112–3123.

34. Miao, L., U. Seifert, M. Wortis, and H.-G. Döbereiner. 1994. Budding transitions of fluid-bilayer vesicles: the effect of area-difference elasticity. *Phys. Rev. E.* 49:5389–5407.

35. Huh, N.-W., N. A. Porter, T. J. McIntosh, and S. A. Simon. 1996. The interaction of polyphenols with bilayers: conditions for increasing bilayer adhesion. *Biophys. J.* 71:3261–3277.

36. Wimley, W. C., and S. H. White. 1996. Experimentally determined hydrophobicity scale for proteins at membrane interfaces. *Nat. Struct. Biol.* 3:842–848.

37. Masum, S. M., S. J. Li, Y. Tamba, Y. Yamashita, T. Tanaka, and M. Yamazaki. 2003. Effect of de novo designed peptides interacting with the lipid-membrane interface on the stability of the cubic phases of the monoolein membrane. *Langmuir.* 19:4745–4753.

38. Lopez-Montero, I., N. Rodriguez, S. Cribier, A. Pohl, M. Velez, and P. F. Devaux. 2005. Rapid transbilayer movement of ceramides in phospholipid vesicles and in human erythrocytes. *J. Biol. Chem.* 280: 25811–25819.

39. Lipowsky, R. 1995. Generic interaction of flexible membranes. *In* Structure and Dynamics of Membranes. R. Lipowsky and E. Sackmann, editors. Elsevier, Amsterdam.

40. Mathivet, L., S. Cribier, and P. F. Devaux. 1996. Shape change and physical properties of giant phospholipid vesicles prepared in the presence of an AC electric field. *Biophys. J.* 70:1112–1121.

41. Marsh, D. 1990. Handbook of lipid bilayer. CRC Press, Boca Raton, FL.

42. Wenk, M. R., and J. Seelig. 1998. Magainin 2 amide interaction with lipid membranes: calorimetric detection of peptide binding and pore formation. *Biochemistry.* 37:3909–3916.

43. Nagle, J. F., and S. Tristram-Nagle. 2000. Structure of lipid bilayers. *Biochim. Biophys. Acta.* 1469:159–195.

44. Masum, S. M., S. J. Li, T. S. Awad, and M. Yamazaki. 2005. Effect of positively charged short peptides on stability of cubic phases of monoolein/dioleoylphosphatidic acid mixtures. *Langmuir.* 21:5290–5297.

45. Furuike, S., T. Ito, and M. Yamazaki. 2001. Mechanical unfolding of single filamin A (ABP-280) molecules detected by atomic force microscopy. *FEBS Lett.* 498:72–75.

46. Toraya, S., T. Nagao, K. Norisada, S. Tuzi, H. Saito, S. Izumi, and A. Naito. 2005. Morphological behavior of lipid bilayers induced by melittin near the phase transition temperature. *Biophys. J.* 89:3214–3222.

47. Inaoka, Y., and M. Yamazaki. 2007. Vesicle fission of giant unilamellar vesicles of liquid-ordered-phase membranes induced by amphiphiles with a single long chain hydrocarbon chain. *Langmuir.* 23:720–728.